# Astronomical Polarimeter and Pulse Timer

David Patenaude (CpE, PSE), Ethan Tomczak (EE), Vincent Miller (PSE), David A. Urrego (CpE)

College of Optics and Photonics, and Dept. of Electrical and Computer Engineering, University of Central Florida, Orlando, Florida, 32816-2450

***Abstract* — Studying the polarization and timing of pulsar emissions provides key insights into neutron stars' magnetic fields, emission mechanisms, and surrounding interactions. Few optical pulsars are known. The Crab Pulsar, known for its rare visible wavelength emission, is a prime candidate for visible spectrum polarimetry. To capture high-resolution data, a Stokes polarimeter system was designed using Wollaston prisms, a rotating half-wave plate, and single photon photodetectors. Controlled by an ESP32 MCU, the system samples data at 500 KSPS, allowing for precise real-time analysis of polarization states. This instrument advances neutron star research, particularly understanding emission dynamics.**

***Index Terms* — Crab Pulsar, Stokes Polarimeter, Polarization Measurement, Pulse Timing, Neutron Stars, Wollaston Prism, High Temporal Resolution.**

## I. Introduction

Pulsars, highly magnetized rotating neutron stars, emit pulsating beams of electromagnetic radiation that can be observed across various wavelengths. These emissions provide a rare opportunity to study extreme physical environments, offering insights into the structure and behavior of neutron stars' intense magnetic fields and rapid rotational dynamics. The Crab Pulsar, located in the Crab Nebula, is one of the most well-studied pulsars due to its pulsed emissions in the visible spectrum, a very rare feature for a pulsar. Its unique characteristics make it an ideal subject for exploring the mechanisms behind pulsar radiation, which can deepen our understanding of neutron star physics and broader astrophysical processes.

To analyze the Crab Pulsar's emissions effectively, we developed a Stokes polarimeter system designed to measure polarization states and pulse timing with high temporal resolution. Accurate polarization measurements help map magnetic field structures, while precise pulse timing can reveal rotational properties and potential irregularities over time. This system utilizes Wollaston prisms to split incoming light into its component polarization states, complemented by a rotating half-wave plate to modulate these states for comprehensive instrumental error correction. Highly sensitive photodetectors capture modulated light, ensuring reliable data capture.

At the core of the system is an ESP32 microcontroller, which manages data collection and processing with up to 500 KSPS sampling rate, facilitating real-time analysis of polarization data. The data handling and processing design emphasizes efficiency to maintain signal integrity and prevent overflow, ensuring accurate and complete data acquisition for astrophysical study. This instrument advances pulsar research by providing a practical, cost-effective means to study neutron stars and their interactions, ultimately contributing to astrophysics and aiding in the broader understanding of these extraordinary celestial objects.

Stokes polarimetry consists of measuring the orthogonal polarization components of light, then comparing the intensities of each. This is used for calculating the Stokes parameters, a set of four numbers that together describe the complete polarization state. Our specific use case only requires measuring linear polarization, and as a result we only calculate the three linear Stokes parameters. This requires us to measure four polarization angles: 0°, 45°, 90°, and 135°.

## II. Design Considerations and Requirements

In this section, we will discuss some of the driving requirements and other considerations that we had to keep in mind when designing our project. The specifications for our project are listed in Table 1. The highlighted rows are the specifications that we will demonstrate. We start by considering the environment that our instrument will be in. As a telescope-mounted instrument, our design must be able to mechanically withstand various rotation states. Telescopes are also not usually climate controlled, and so we must ensure there are no issues that arise from this.

Since our goal is to measure the polarization of faint light from far away objects, we specify the required sensitivity of our detectors and the desired accuracy of polarization measurement, specified in Table 1. Data handling of up to 8 MB/s would be required for 1 MHz sampling. Since the implementation of a file system slows down storage media, we aim to sample at 500 kHz generating 4 MB/s of data. We also want the ensure the end-user does not have to wait a long time between samples. The main limitation here would be the exporting of data over UART to Python, which is slow.

Final implementation is intended for the telescope at UCF's Robinson Observatory. This is 20" telescope with a 4165 mm focal length (f/8.2). These parameters together determine the shape of all incoming light to the system.

Our selection of components to use for this project stem from the above considerations and requirements. Our important component selections are the microcontroller (MCU), photodetector, type of op-amp, and storage solution. Our other selection comparisons follow a similar process to the ones highlighted here.

For controlling our instrument, there are a couple of options, such as a field-programmable gate array (FPGA) or an MCU. While FPGAs have some benefits, our project involves many peripherals that an MCU has built-in. Our MCU has an analog-to-digital converter, PWM motor controller, and, SD card protocol support all included.

We chose our photodetector by considering our requirement to detect very weak optical signals, in combination with budgetary constraints. Light from neutron stars is quite faint in comparison to that of normal stars. As such, we require detectors that are capable of single-photon counting for visible light. The ideal products for this are prohibitively expensive, however a compromise product balancing noise and cost was found in the Thorlabs PDA series of Silicon Photomultiplier detectors.

Our choice of half waveplate was determined solely by the wavelength dependent retardance error of available products. While electrically modulable waveplates are mechanically simpler, they have an unacceptably high variation in performance with respect to wavelength. As such, we decided to use a standard achromatic waveplate, and mechanically rotate it instead.

For selecting our op-amps, our main concern is preserving signal integrity. Our main criteria for this is looking for low noise op-amps with a high slew rate to capture a fast-changing signal. Additionally, with the detectors signal characterization we must have an amp with a high gain bandwidth product to allow the full signal through. The detectors can produce pulses within the MHz range. Our choice of op amp was the TI OPA140AIDBVR which meets our criteria.

When determining what storage solution to use, there were a few options. With the MCU chosen, we could add memory (PSRAM) or flash, but these either lack the capacity or speed that is required. Since the MCU supports 4-bit SD card reading and writing, we decide on implementing fast, bulk storage via a microSD card.

TABLE I
PROJECT SPECIFICATIONS

| Description | Specification |
|---|---|
| **Optical Power Sensitivity** | < 1 pW |
| **Down time between samples** | 15 seconds or less |
| **Imaging System Magnification** | Magnifications of 0.8 and 0.018 |
| 4 Output PSU | 3.3V, 5V, ±12V |
| Sample rate of pulse counting | 500 kHz |
| Minimum sample duration/time | 100ms |
| Polarization Measurement | Accurate to 1° |
| External memory size | 4GB |
| Instrument size | 20"x20"x10" |
| Internal data rate capacity | At least 4 MB/s |
| Analog Frontend Speed | 1 GHz or better |

## III. SYSTEM ARCHITECTURE

The Crab pulsar polarimeter and pulse timer system architecture is organized into distinct subsystems, each tailored to meet specific project requirements for data acquisition, processing, and storage. The architecture is divided into three main components: the optical system, data acquisition and processing unit, and power management system, shown as blocks in Fig. 1. Together, these subsystems enable high-resolution capture and analysis of the Crab Pulsar's polarization and pulse timing data.

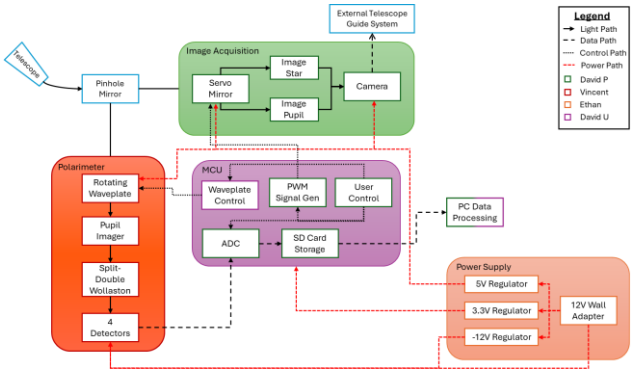


Fig. 1. Block diagram of our project design. Colored boxes are the different subsystems, with more details contained within them.

### A. Optical System

Within the optical design, there are two distinct subsystems, the linear Stokes' polarimeter, and the image acquisition system. The actual instrument is designed as a linear Stokes' polarimeter to measure the polarization of the incoming light in one shot. Normally, polarization is measured by rotating a polarizer and observing the changes in intensity, but with a Stokes' polarimeter, the polarization is measured in one shot by using multiple detectors. Polarimetry of a source with unknown and variable polarization could not be easily performed without single shot measurements. The other optical system is the image acquisition system. This system is used to image the object of interest, which can then be sent to the telescope's guide system. Additionally, the acquisition system can switch to imaging the telescope's aperture, providing the exit pupil of the telescope. The exit pupil is useful when aligning the instrument with the telescope.

To separate light between subsystems, we have designed a custom-made lithographic pinhole mirror. This is a metallic mirror with a 122 µm elliptical hole etched into its center, allowing a specific target star to pass through for scientific measurements, while all other light is redirected for use in telescope guiding. For testing and demonstration purposes, we use a configuration with distinct mirror and pinhole optics.

#### 1. Polarimeter Design

Effective stokes polarimetry requires efficient splitting of light among the four detectors. We accomplish this by using a split mirror located at the system pupil. Placing this mirror system at the pupil ensures that all collected light is evenly distributed to each half of the Stokes polarimeter. Splitting at the pupil has the added benefit of negating the effects of atmospheric turbulence introducing jitter to starlight over the short term. After splitting both beams pass through a Wollaston prism, splitting it into orthogonal polarization components. Each component is then measured by a separate photodetector.

Focal lengths were determined through considering the telescope's f/8.2 input, in addition to our goal to minimize the overall instrument size. The chosen focal lengths are the smallest possible while remaining mechanically feasible and realistic for construction. Using equation (1), we calculated the collimated beam diameter for the pupil splitting module. Additionally, this tells us the position of the system pupil and therefore the location of the pupil splitting mirrors.

$$f/_{\#} = \frac{EFL}{D} \quad (1)$$

The two Wollaston prisms are oriented at 45 degrees to each other, allowing us to collect the needed measurements for Stokes polarimetry. The prisms themselves are AR coated calcite, with an output beam divergence angle of 20 degrees. These were chosen for their large divergence angle and high transmission of visible light. Initial polarimeter designs instead used a Wedged Double Wollaston Prism, which cleverly combines the pupil splitting mirror and two Wollaston prisms into a single custom optic. While this is the ideal solution, it was not possible to implement due to manufacturer restrictions, and the two-Wollaston design was created to replace this.

All photodetectors have variations in response over the effective detecting area, which is a potential source of error in any collected data. To account for this the system pupil is reimaged onto the detector. This has the benefit of providing wide beam coverage over the detector, while additionally minimizing any movement of the image across the surface. The incident beam diameter was designed to be close to that of the detector (1.3 mm), ensuring that all measurements are taken using a consistent average responsivity. Beam diameters are intentionally undersized however, to prevent losing signal due to mechanical changes in the system causing light to miss the detector.

Reimaging the pupil onto each detector requires beam shrinking optics to reduce beam diameter to be near the detector width. This is done again using (1) to construct a Keplerian beam expander, operating in reverse, with the input and target final beam diameters taken into consideration. Lenses are then chosen that will match the required focal lengths as closely as possible, allowing for some flexibility in the final beam diameter.

Further considerations are the affect optics will have on incident light. Instrumental polarization effects can be partially corrected through calibration, but this is unable to account for gradual changes that occur over the course of operation. We correct for instrumental polarization using a half wave plate, constantly rotating at 1Hz, located before all other polarimeter optics.

TABLE II
POLARIMETER SYSTEM PERFORMANCE

| Specification | Value |
|---|---|
| Pupil Image Diameter | 935 µm |
| Detector Area Coverage | 71.9% |
| Wavelength Dependent Area Variation | 12.1 µm |
| Pupil Image Position Variation | 3 µm |

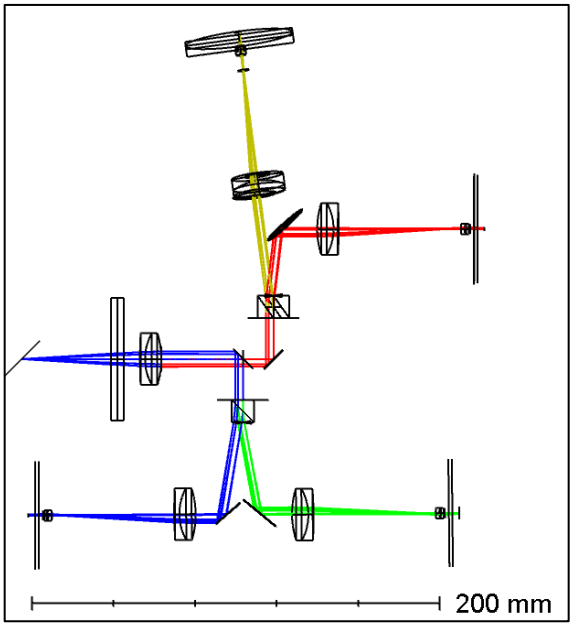


Fig. 2. *Zemax* layout of the polarimeter system, with rays entering from the center right. Blue and green paths correspond to 0º and 90º polarizations, red and yellow correspond to 45º and 135º, respectively.

Performance is measured in Table II using the average across the four polarimeter arms, though little variation is seen between individual data points.

*2. Image Acquisition Design*

As mentioned, the image acquisition system consists of two functions. The primary function is to image the star, or other celestial body, for the telescope's tracking system, also known as a guide system. The secondary function is to image the exit pupil of the telescope which is used to ensure proper alignment of the instrument with the telescope. The main specifications and requirements for this system are shown in Table 3. The main optical design tool we use is *Zemax* after we perform paraxial calculations by hand. With the guide camera selected, we were able to determine the magnification requirements so that the images would fit onto the camera's detector. We define that the star imaging path is the one that reimages the telescope's output image onto the detector and the pupil imaging path as the one that images the telescope's aperture to the detector. The main paraxial equations used in our design include:

$$\frac{1}{f} = \frac{1}{u} + \frac{1}{v} \tag{2}$$

$$m = \frac{h'}{h} = \frac{v}{u} \tag{3}$$

$$\frac{1}{f_{sys}} = \frac{1}{f_1} + \frac{1}{f_2} - \frac{d}{f_1 f_2}. \tag{4}$$

TABLE III
SUMMARY OF IMAGING SYSTEM SPECIFICATIONS

| Specification | Value |
|---|---|
| Field of View (FOV) | 4 arcminutes |
| Chromatic Aberration | Near diffraction-limited |
| Star Magnification | 0.867 |
| Pupil Magnification | 0.0189 |

The first step of the paraxial design is to determine the approximate locations of the lenses. To minimize aberrations, more than one lens will be used for each path, that way the light bending is split between the lenses to reduce aberrations. The distances can be found from knowing the desired magnification and the focal lengths of the lenses, by using eq. (2) and (3). Since there are a lot of free variables, and we are trying to find the focal lengths, we are free to select a focal length for the star imaging path. From this one focal length selection, we can use Gullstrand's equation (4) to split a single lens into two lenses. With the star imaging path decided, the total distance that the pupil imaging path can occupy is known. This provides us enough information to find the focal lengths for the rest of the lenses, using eq. (2) and (3). The final design is shown in Fig. 3.

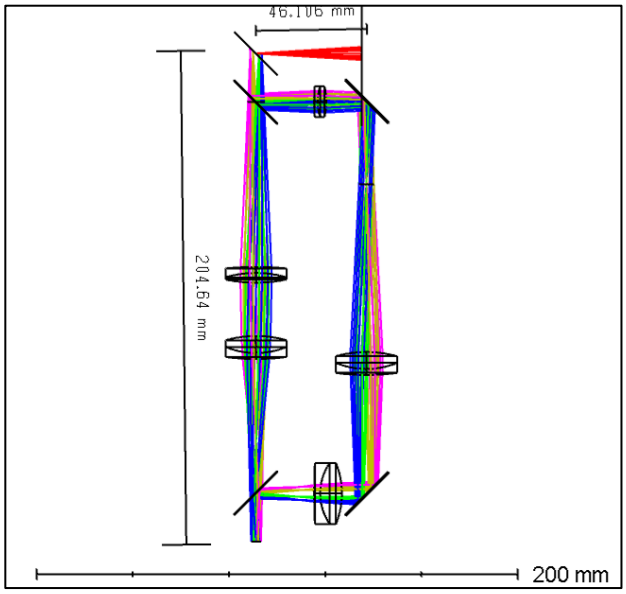


Fig. 3. *Zemax* layout of image acquisition system. The full-FOV is traced, where each color is a different field angle. The total area is around 60 mm by 220 mm.

By designing with multiple paraxial lenses, when we switched to using real, off-the-shelf lenses, the overall aberrations were under control. We evaluate the performance of the optical system by using both the spot diagram and the Seidel coefficient report in *Zemax*. These provide the simulated size of a spot in microns and how aberrated the light's wavefront is, in terms of wavelength. Table 4 provides the numerical results obtained from *Zemax*, for the 1' and 2' fields. The wavelength in the table is the primary wavelength, at 588 nm.

TABLE IV
PERFORMANCE OF IMAGING SYSTEM

| Metric | 1' field | 2' field |
|---|---|---|
| RMS Spot Size | 4.408 µm | 6.3 µm |
| Diff-Limit Spot Size | 5.043 µm | 5.043 µm |
| Chromatic Focal Shift | 214.95 µm (Diff-Limit: 116 µm) | |
| Spherical Aberration | 0.377 λ | |
| Coma | -0.367 λ | |
| Astigmatism | 0.457 λ | |

*B. Data Acquisition and Processing Unit*

Data acquisition and processing are handled by the ESP32 microcontroller, selected for its capability to support high-speed data transfer and low-latency processing. The ESP32 is equipped with an ADC operating at a maximum of 2 MSPS sampling rate, which is essential for capturing the granular details of the pulse timing of the Crab Pulsar. The microcontroller runs software developed using the ESP-IDF (Espressif IoT Development Framework). Using Python enables us to process data in near-real-time.

A custom state machine within the ESP32 software manages data flow, controlling sampling intervals, data buffering, and transmission. Fig. 4 shows a detailed flowchart of the sampling process. The ADC samples polarization data from the photodetectors, which is then processed to extract the Stokes parameters in Python. Data from the polarimeter is stored temporarily in ring buffers within PSRAM, preventing data overflow during sampling. The data is transferred to the microSD card for storage before the buffer can overflow, ensuring the continuity of high-resolution data.

Fourier transforms are applied to the raw data, enabling detailed frequency analysis of the pulsar's signal. This analysis provides insights into pulse timing characteristics and any frequency-dependent variations in polarization. The processed data can be accessed in near-real-time, allowing researchers to monitor the Crab Pulsar's emission patterns during a sampling session.

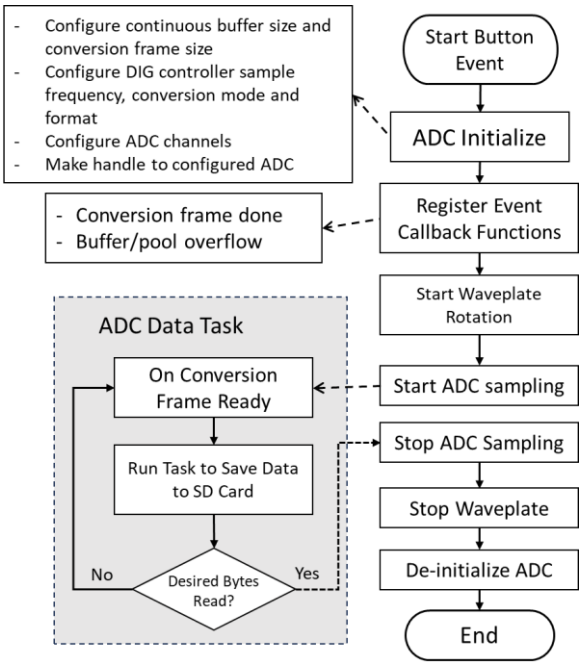


Fig. 4. Flow of events when MCU collects a sample from the ADC.

*C. Hardware Subsystems*

The telescope polarimeter and pulse timer project relies on a robust electronics system to manage data acquisition, user input, and signal processing for precise polarization measurements. The key components in this setup are the power supply unit (PSU), analog front-end (AFE), and microcontroller unit (MCU).

*1. Power Supply Unit (PSU)*

To maintain stable voltage levels across the system, the PSU operates from a 12V, 7A wall adapter, with voltage regulation achieved by Texas Instruments' LM2675ADJ for 3.3V and 5V outputs and Analog Devices' MAX17577 for -12V. A single LM2675ADJ circuit supplies stable 3.3V and 5V outputs, each providing up to 1 A. The 5V output powers both the offset signal for the analog front end (AFE) and the waveplate rotation mount, which can draw up to 800 mA at peak operation.

For the -12V requirements of peripheral components, including 4 photodetectors and 16 op-amps on the peripherals board, two MAX17577 circuits are configured in parallel, delivering up to 600 mA. A +12V line is also directly supplied from the 12V input, supporting the same components as the -12V line. To ensure system safety, a current protection measure of 1A is implemented on the +12V line to prevent overload.

This configuration ensures adequate current for all signal conditioning stages in the AFE, maintaining reliable functionality across the system. The unit does not include a power switch, so it remains fully operational whenever the 12V wall adapter is connected, providing continuous functionality as long as external power is supplied.

*2. Analog Front-End (AFE)*

The AFE processes incoming low-level signals from the photodetector sensors and prepares them for digital conversion by offsetting the detector signal 0.2V making it sampleable by the ESP ADC. The design includes both signal processing and noise reduction. For signal processing, the TI OPA140AIDBVR op-amps are selected for their high slew rate (20 V/µs), low noise (5.1 nV/√Hz), and wide supply voltage range (4-36V). This enables precise amplification and conditioning of weak signals from photodetectors. The op-amps' high gain-bandwidth product (11 MHz) ensures that the signals retain fidelity across a broad frequency range, allowing the system to capture fast, subtle changes in the incoming light signal. The AFE circuit is shown in Fig. 5.

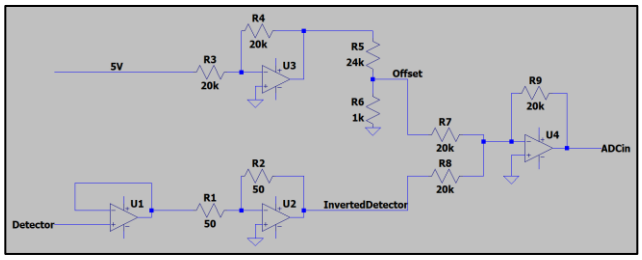


Fig. 5. LTSpice schematic of the analog front-end (AFE). The detector input is offset to be within range of the MCU's ADC.

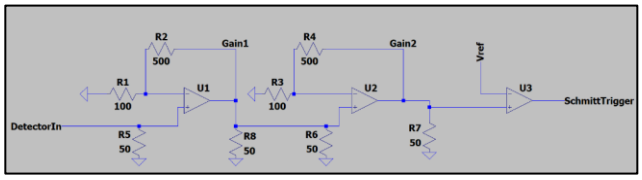


Fig. 6. LTSpice schematic of the analog front-end (AFE). The detector input is amplified to be read by the MCU Trigger.

Late in the development process, we redesigned the signal amplification for the PDA44 photodetector by selecting the OPA847, an ultra-fast amplifier with a gain-bandwidth product of 3.9 GHz. This change was driven by the need to reliably handle the detector's output pulses, which are 4 ns in duration, 50 mV in amplitude, and occur at a 5 kHz frequency during dark counts. The high-speed performance of the OPA847 ensures that these rapid, low-voltage pulses are faithfully amplified with minimal distortion, preserving their shape and fidelity for accurate analysis. This late-stage redesign reflects our commitment to achieving the highest possible signal accuracy.

*3. Microcontroller Unit (MCU)*

The MCU is central to managing data acquisition and interfacing with both the user and external storage. Its key functions include data acquisition, a user control interface, and data input and output.

For data acquisition, the built-in ADC samples at 500 kHz, enabling high-resolution temporal data capture needed for pulsar timing. The high-speed ADC converts analog signals from the AFE into digital data, which is then stored in 4 GB or more of SD card memory, supporting approximately 500 one second samples.

For the user control interface, the MCU is configured to handle direct user input through physical controls such as buttons, dials, and an LCD display. Users can adjust sampling rates (100 kHz to 1 MHz) and sampling duration (from 25 ms to 1 s). This configurability allows for flexible data capture tailored to various observational needs.

To support data input and output, our MCU board includes USB 2.0 connectivity, facilitating data export to an external computer for post-processing. This interface also allows for initial programming and reconfiguration of settings, streamlining setup and operation.

*D. Data Storage and Output*

The system's microSD card is critical for handling the large volumes of data generated by a high sampling rate. The microSD storage is configured to allow for uninterrupted data logging, even during extended observation sessions. This setup not only enables efficient data storage but also facilitates data transfer for post-observation analysis.

The output data, including processed polarization states and pulse timing metrics, can be transmitted to external systems for further analysis. The ESP32's UART capability supports communication with external devices, allowing for easy data retrieval to the PC, and communication with the rotation mount.

## IV. IMPLEMENTATION

The implementation of the Crab Pulsar Polarimeter and Pulse Timer involved extensive integration of hardware, software, and optical components to ensure precision in data collection and processing. Each component was chosen and calibrated to meet the requirements for high-

speed, high-accuracy data acquisition and real-time analysis of the Crab Pulsar's emissions.

### *A. Optical Component Assembly*

To ensure proper alignment of optical components, care must be taken when designing the mounts for our lenses and mirrors. Due to size constraints of 3D printed parts and concerns about the flexibility of wood, it was determined that a machined aluminum base would be best for the polarimeter assembly, shown in Fig. 6. All parts then have 3D printed mounts that can be screwed directly into the correct locations, allowing for minor adjustments as needed.

For the image acquisition assembly, a base was designed in SolidWorks and then 3D printed. The base has mounts for all the lenses and mirrors, as well as the guide camera. The mounts are designed to allow minor, by-hand adjustments along the path of the light. The printed assembly is shown in Fig. 7.

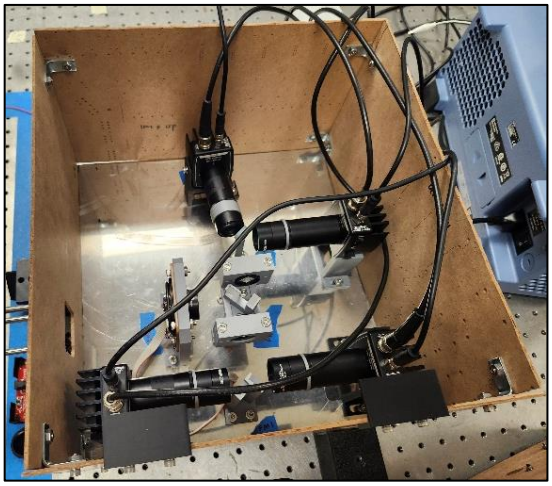

Fig. 7. Polarimeter assembly with all optics included and mounted to an aluminum baseplate. A cardboard enclosure is included to limit ambient light affecting measurements during testing.

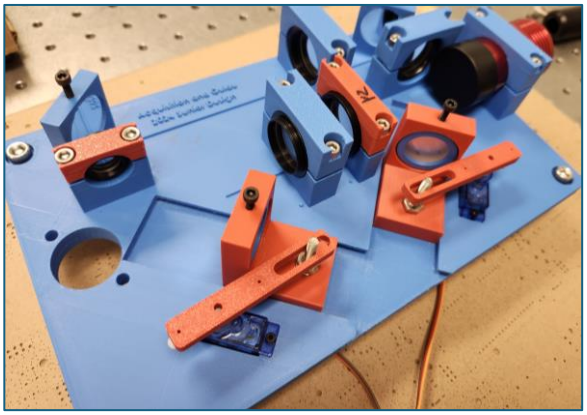

Fig. 8. Image of printed image acquisition mounting base. Two servos are used to slide mirrors along the cut outs.

### *B. Embedded Software and Data Processing*

The ESP32 microcontroller's embedded software was developed in ESP-IDF, allowing for optimized performance. The core of the software is a state machine that manages data flow from the ADC to the storage devices. This state machine controls sampling intervals, processes polarization data from the ADC, and directs data to the 64 GB microSD card.

Fourier transforms are applied to the raw ADC data which enables frequency analysis of the Crab Pulsar's emission patterns. This data processing method helps isolate specific frequencies and their associated polarization states, providing deeper insights into the pulsar's characteristics. The software also uses error-checking protocols to validate data integrity, with any discrepancies flagged for further review.

Python scripts complement the ESP32's embedded software, facilitating data handling and post-processing on external devices. The Python package supports analysis of pulse timing data, polarization calculations, and visualization, making it easier for researchers to interpret the collected data. Additionally, real-time monitoring scripts allow for continuous observation of the microcontroller, alerting researchers to any anomalies in data capture or signal stability.

### *C. Data Storage and Buffering*

Data is stored on a microSD card because it is the fastest bulk storage option that works well with a microcontroller. A filesystem is mounted on the card for easier processing of data. The alternative to a filesystem would be raw memory access, which would improve the speed of transfers at the cost of additional bookkeeping by the programmer. A sample's data is saved as a series of data

files (.dat) in a unique folder for each sample. Metadata is stored in a log file with the sample's name, which includes the bytes read for each file, the sample frequency, and, sample duration. During testing, we discovered that the SD card, while rated for higher write speeds, was limited to around 7 MB/s writes when using a file system. This restricts the maximum sampling frequency before the internal ADC buffers overflow and data is lost. Since continuous data is necessary in this application, data loss must be avoided at all costs.

### *D. Power Supply and Stability*

The power supply for the polarimeter and pulse timer is designed to provide stable, efficient voltage regulation across the system. The main input is a 12V wall adapter delivering up to 7 A, regulated to meet the specific needs of each component to ensure steady operation and accurate data capture.

The 3.3V and 5V regulators play a crucial role in powering the core and peripheral devices. The 3.3V output powers the ESP32 and user interface components, supporting reliable data acquisition and user interaction. The 5V regulator supplies power to the rotation mount, which controls the waveplate's rotation for polarization adjustments, as well as the offset signal for the analog front end (AFE), aiding in consistent signal processing.

For signal detection and processing, the ±12V supplies both the OPA140 op-amps in the AFE and the PDA44 photodetectors. These voltages ensure that the op-amps operate with high stability and low noise, essential for capturing high-fidelity polarization data. The PDA44 photodetectors, also powered by ±12V, accurately measure light signals, which are then processed in the AFE before sampling by the ESP32's ADC.

This integrated power approach distributes current effectively across all connected devices, allowing each to operate within its specified range without interference. By maintaining regulated, isolated power rails for each voltage level, the system maximizes signal fidelity, ensuring that the Crab Pulsar's emissions are captured with precision and reliability.

### *E. Calibration and Integration*

In the integration of the power and control systems, we designed the 3.3V and 5V regulators on a separate breakout board, isolated from the -12V regulator. This setup was chosen to avoid assembly complications, as the -12V regulator chip has an extremely compact footprint that can be difficult to manage on larger boards, especially if reworking is required after testing. The same approach was applied to the ESP32 Mini microcontroller by placing it on its own breakout board, making it easier to troubleshoot or replace if needed.

The peripherals, user controls, detector inputs, wave plate rotation mount, and analog front end (AFE) module were consolidated on a larger board. This peripheral board includes a jumper that connects to the MCU breakout board, allowing for interconnectivity across the system.

## V. TESTING AND VALIDATION

To test our design, we recreate an f/8.2 beam to mimic the telescope in the Robinson Observatory at UCF. To make a suitably dim source of light, we use a series of neutral density (ND) filters after using crossed polarizers. The combination of these enables us to test using optical powers at or below a nanowatt, in combination with a polarization. An optical chopper is used to simulate a pulsing effect to add further realism to our testing. Measurements of dark count rate and photon count rate from sample light sources have been taken using a pulse counting mode on laboratory oscilloscopes. Using these methods, we created a 10 fW vertically polarized input beam. With this, we should be able to detect approximately 26,000 photons per second. Our measurements were closely in line with this expectation after accounting for the effects of background light.

Testing the imaging system began by aligning the object to the image plane without the camera to make the process easier. The alignments are done by hand and with the eye. Once complete, the camera is added back, and it is aligned to get the most in-focus image. Using a ruler, the magnification of the two imaging paths can be found. We were able to show that both paths had 3% or less error in magnification. The star imaging path's magnification was 0.837 (vs. 0.863) and the pupil imaging path's magnification was 0.0186 (vs. 0.0189). With magnification slightly less than the designed, the images will fit onto the detector without any problems.

Before integrating the different subsystems, we test each subsection individually. The MCU is tested using a simple photodiode, before being hooked up to the photodetectors used in the project to ensure that the data is collected and stored as expected. Sending the data to a waiting Python program is also tested beforehand in this process. The optics are tested by measuring the magnification to ensure proper imaging is taking place. Polarization accuracy is checked by using a known source of light to compare with the output of our data processing suite. The power supply boards are tested by ensuring that they supply a constant voltage for any given load. Conveniently, there is test equipment that can provide a load for the power supplies for testing. The MCU board is tested by flashing a simple

program at first, and then our actual program. If debugging is necessary, we start by checking continuity of our connections, and then we check the voltage. After verifying the hardware connections, we look to the relevant portion of software to determine if there are any bugs.

Once all subsystems are tested, we pieced them together, where we performed testing of performance and functionality. Further calibration steps will involve using a broad-spectrum laser emitting across the entire visible spectrum, to more accurately simulate real starlight.

For the initial testing phase, we verified the 3.3V and 5V regulators in conjunction with the MCU board to ensure that power flowed correctly and that the regulators supplied the required voltages and currents. This step confirmed that the MCU could be successfully powered. The regulators were also tested with the peripherals board to validate proper operation of the AFE module. Finally, we integrated all components—the 3.3V and 5V regulators, -12V regulator, MCU board, and peripherals board—to confirm system-wide functionality.

As a last step, we tested power delivery to the photodetectors, initially using a spare detector to verify that the dual voltage inputs (+12V and -12V) were stable and functional, ensuring safe operation for the entire detection system. This structured approach allowed us to systematically test and confirm the functionality of each component before full integration, ensuring a robust and reliable system.

## VI. Conclusion

In summary, we have designed a polarimeter to measure the polarization of faint light from astronomical objects, while also being able to measure the temporal characteristics. Of particular interest is the Crab pulsar, where we can measure the pulse times and polarization concurrently at visible wavelengths. Pulsars are not well understood, and it is our hope that astronomers and astrophysicists can utilize our instrument to potentially discover more about these fascinating celestial objects.

By utilized our knowledge bases in optics, electronics, and software, we were able to plan, develop, integrate, and test this technically challenging project. In the process, we had to learn the best way to mechanically arrange and mount our components and subassemblies. Through our perseverance and hard work, we were able to overcome many obstacles to deliver this project under the tight deadlines of senior design. We look forward to bringing our experiences gained into the next chapters of our careers.


## Acknowledgements

The authors would like to acknowledge our project's sponsor, Dr. Stephen Eikenberry for his support and for making this project a possibility. We also thank Dr. Leland Nordin for his generous support in providing equipment for testing and evaluation.


## Biographies

**Vincent Miller** is a Photonic Engineering student at the University of Central Florida. He plans to pursue a PhD in photonics after graduation.

**David Patenaude** is a Photonic Engineering and Computer Engineering student at the University of Central Florida. He intends to pursue a job in the computer hardware or optics & photonics industry but is also considering a PhD in Optics.

**Ethan Tomczak** is an Electrical Engineering student at the University of Central Florida. After graduation, he intends to work in the field of analog signal processing and system design

**David Urrego is a Computer Engineering student** at the University of Central Florida. He aims to apply his technical skills in a career in reliability, system safety, or computer engineering.